A single domain intrabody targeting the follicle-stimulating hormone receptor (FSHR) impacts FSH-induced G protein-dependent signalling

Pauline Raynaud[1], Vinesh Jugnarain[1], Océane Vaugrente[1], Amandine Vallet[1], Thomas Boulo[1], Camille Gauthier[1], Asuka Inoue[3], Nathalie Sibille[4], Christophe Gauthier[1], Frédéric Jean-Alphonse[1,2], Eric Reiter[1,2], Pascale Crépieux[1,2]*, Gilles Bruneau[1]*

[1]Physiologie de la Reproduction et des Comportements (PRC), Institut National de Recherche pour l'Agriculture, l'Alimentation et l'Environnement (INRAE), Centre National de la Recherche Scientifique (CNRS), Institut Français du Cheval et de l'Equitation (IFCE), Université de Tours, 37380 Nouzilly, France

[2]Inria, Inria Saclay-Ile-de-France, 91120 Palaiseau, France

[3]Graduate School of Pharmaceutical Sciences, Tohoku University, Sendai, Japan

[4]Centre de Biologie Structurale (CBS), CNRS, University Montpellier, Inserm, Montpellier, France

*Corresponding authors:

Dr. Gilles Bruneau, UMR Physiologie de la Reproduction et des Comportements, Centre de Recherches INRAE Val de Loire, F-37380 Nouzilly, France. E-mail: Gilles.Bruneau@inrae.fr

Dr. Pascale Crépieux, UMR Physiologie de la Reproduction et des Comportements, Centre de Recherches INRAE Val de Loire, F-37380 Nouzilly, France. E-mail: Pascale.Crepieux@inrae.fr

Abstract

Intracellular variable fragments from heavy-chain antibody from camelids (intra-VHH) have been successfully used as chaperones to solve the 3D structure of active G protein-coupled receptors bound to their transducers. However, their effect on signalling has been poorly explored, although they may provide a better understanding on the relationships between receptor conformation and activity. Here, we isolated and characterized iPRC1, the first intra-VHH recognizing a member of the large glycoprotein hormone receptors family, the follicle-stimulating hormone receptor (FSHR). This intra-VHH recognizes the FSHR 3rd intracellular loop and decreases cAMP production in response to FSH, without altering Gαs recruitment. Hence, iPRC1 behaves as an allosteric modulator and provides a new tool to complete structure/activity studies performed so far on this receptor.

Keywords: G protein-coupled receptors, FSH receptor, intracellular VHH, cell signalling

39 **Abbreviations**

40 GPCR: G protein-coupled receptor

41 FSH: Follicle-stimulating hormone

42 FSHR: FSH receptor

43 LHCGR: Luteinizing hormone/choriogonadotropin receptor

44 TSHR: Thyroid-stimulating hormone

45 BSA: Bovine serum albumin

46 BRET: Bioluminescence resonance energy transfer

47 HTRF: Homogeneous time-resolved fluorescence

48 ICL: intracellular loop

49 AVP: Arginine-vasopressin

50 AVPR2: Arginine-vasopressin 2 receptor

51 ISO: Isoproterenol hydrochloride

52 ADRB2: β2 adrenergic receptor

53 Fsk: Forskolin

54 PBS: Phosphate-buffered saline

55 RLuc8: luciferase from the sea pansy *Renilla reniformis*

56 mGs: Mini Gs protein, minimal engineered GTPase domain of the Gα subunit

57 APC: Allophycocyanine

58 HEK293: Human Embryonic Kidney 293

Introduction

G protein-coupled receptors (GPCRs) represent a large family of membrane receptors characterized by an N-terminal extracellular domain, seven transmembrane domains connected by three extracellular and three intracellular loops, and an intracellular C-terminal domain. Ligand binding to a GPCR leads to conformational changes within the transmembrane and intracellular domains, mediating the transduction of an extracellular signal to the interior of the cell. GPCRs are highly dynamic proteins, adopting a plethora of active and inactive conformations (1). This is in accordance with the fact that, upon ligand binding, they are able to interact with a diversity of downstream signalling proteins with variable efficacy. The signal is transduced by heterotrimeric G proteins (Gs, Gi/o, Gq/11, G12/13), G protein-coupled receptor kinases (GRK) and β-arrestins among others. Since GPCRs are involved in the regulation of numerous physiological and pathological processes, regulating their biological activity has been the object of considerable efforts, involving the use of a variety of molecular tools. Ligands recognizing the orthosteric binding site of a GPCR act as agonists or antagonists. The use of allosteric modulators that favour either active (positive allosteric modulator) or inactive (negative allosteric modulator) conformations may fine-tune GPCR signalling. Biased ligands, whether orthosteric or allosteric, exhibit altered efficacy or potency to regulate a specific signalling pathway, when compared to a reference ligand, providing valuable tools to study and control GPCR signalling regulation.

Small molecules have been extensively explored to modulate GPCR signalling and pharmacology, including the FSHR's (2). In the last decade, there has been a growing interest in the development of antibodies targeting GPCRs, especially in the VHH (VH of heavy chain only antibodies) format. These VHHs of low molecular weight (~13 kDa), display the smallest paratope capable of specifically recognizing an epitope. A long and flexible CDR3 that compensates for the absence of light chain enables them to access and recognize cryptic epitopes, such as binding pockets (3). Furthermore, their conformational stability is an advantageous property. VHHs have disulphide bonds not essential for epitope recognition (4), hence they are especially well-suited for intracellular expression despite reducing conditions in the cytosol.

Ligand-bound GPCRs are structurally instable, and the recruitment of transduction proteins (G proteins, β-arrestins) each stabilize a discrete subset of receptor

92 conformations (5). Similarly, intracellular VHHs (intra-VHHs) have the ability to stabilize
93 selective GPCR conformations. Therefore, intra-VHHs targeting GPCRs have been a
94 tremendous help to solve crystal structures of numerous active GPCRs. For example,
95 Nb80 was used as a chaperone to solve crystal structure of the active beta 2
96 adrenergic receptor (ADRB2) (6), Nb9-8 for the structure of active muscarinic
97 acetylcholine receptor M2 (7), or Nb39 for the active structure of mu-opioid receptor
98 (8). All of these intra-VHHs exhibit G protein mimetic properties. Intra-VHHs stabilising
99 partially active conformations of GPCRs have also been identified, such as Nb71
100 targeting ADRB2 (9). Others were able to stabilize inactive conformations, as Nb60,
101 which acts as a negative allosteric modulator at the ADRB2 (10). In addition, some
102 intra-VHHs have been used as biosensors to track GPCR intracellular trafficking. For
103 instance, Nb80 fused to GFP as a biosensor for ADRB2 activation, revealed that active
104 ADRB2 is present at the endosomes (11). Overall, by providing important stabilizing
105 tools, intra-VHHs allowed valuable structural insights on GPCR activation. However,
106 their modulatory impact on GPCR functioning has been poorly explored. So far, few
107 studies reported a functional allosteric effect of intra-VHHs on GPCR signalling, and
108 they are all directed against five GPCRs only (OPRK1, OPRD1, OPEM1, ADRB2 and
109 US28), amongst the 800 members of the family (for review see Raynaud et al., 2022
110 (12)). For example, eighteen intra-VHHs selected on ADRB2 have been functionally
111 characterized and they display variable inhibitory effects on cAMP production and β-
112 arrestin recruitment (13). Four others inhibited the cAMP-responsive element (14).
113 Intra-VHHs used as regulators of GPCR function can provide insight on GPCR
114 signalling and on the receptor regions that are involved.

115 The follicle-stimulating hormone receptor (FSHR) is a class A (rhodopsin-like) GPCR
116 playing a key role in reproduction, by regulating gametogenesis in male and female
117 (15). The FSHR, together with the luteinizing hormone/choriogonadotropin (LHCGR)
118 and thyroid stimulating hormone receptors (TSHR), constitute the subfamily of
119 glycoprotein hormone receptors. Unlike other class A GPCRs, these three receptors
120 are characterized by a large horseshoe-shaped extra-cellular domain, comprising the
121 hormone binding domain (16). The FSH-stimulated FSHR primarily signals through
122 Gs, the Gαs subunit leading to the production of the cAMP second messenger, thus
123 activating protein kinase A (PKA). The Gβγ subunits activate GRKs, which
124 subsequently phosphorylate the receptor on specific motifs, leading notably to the

recruitment of β-arrestins (17–19). The latter play a key role in receptor desensitization, internalization and recycling, but also in G protein-independent signalling. FSH-activated FSHR is also engaged with other interaction partners (20), and induces a complex signalling network (21).

Through its biological role, the FSHR is a potential target for non-hormonal alternatives to fertility treatments or contraceptives, with the aim of optimizing efficacy while reducing side effects. However, it is not yet clearly understood how a specific signalling pathway correlates with the induced physiological effect. Therefore, to be able to fine-tune FSHR signalling, there is a need for tools allowing to decipher the complexity of the FSHR signalling network. In this study, we isolated a VHH targeting the 3rd intracellular loop of the FSHR, expressed it as an intra-VHH in mammalian cells, showed its binding to the FSHR, and explored its potential modulatory effect on the FSH-induced Gs signalling pathway.

139 **Materials and methods**

140 References of the materials are provided in Supplementary Table 1.
141 Commonly used methods i.e. cell imaging, flow cytometry, VHH production and
142 purification, BRET assays and cAMP measurement, are described in the
143 supplementary methods section.

144 - *Phage library*

145 The phage library was obtained after intramuscular immunisation of llama with a cDNA
146 encoding the human FSHR (In-Cell-Art, Nantes, France). Total RNAs were extracted
147 from llama circulating leukocytes using LeukoLOCK™ Fractionation & Stabilization Kit
148 (Invitrogen, Waltham, Massachusetts, USA) and reverse-transcribed as cDNA using
149 SuperScript™ III Reverse Transcriptase (Thermo Fisher Scientific, Waltham,
150 Massachusetts, USA). VHHs cDNAs were amplified by nested PCR using Platinum™
151 Taq DNA Polymerase (Thermo Fisher Scientific), as described in Supplementary
152 Figure 1. PCR products were inserted between the SfiI and NotI sites of the pCANTAB
153 6 phagemid vector (kindly provided by Pierre Martineau). The resulting recombinant
154 phagemids were transformed in *E. coli* TG1 bacteria (Lucigen, Teddington, UK).
155 Addition of the KM13 helper phage (kindly provided by Pierre Martineau) allowed the
156 production of the phages. The primary library contains 3.10^8 independent phages.

157 - *Phage display*

158 Intra-VHH selection was performed by phage display on each of the three peptides
159 corresponding to the intracellular loops of the human FSHR (ICL1, ICL2 and ICL3).
160 ICL1 (TTSQYKLTVPR), ICL2 (ERWHTITHAMQLDCKVQLRH) and ICL3
161 (HIYLTVRNPNIVSSSSDTRIAKR) peptides were synthetized by Genecust (Boynes,
162 France). Three selection rounds were carried out. For each round of selection, 1 µg of
163 peptide in phosphate-buffered saline (PBS) pH 7.4 was coated into the selection well
164 of Nunc MAXISORP strips (Dutscher, Bernolsheim, France). The first round started
165 with a sample of 10^{11} to 10^{12} phages from the amplified phage library. Aspecific phages
166 depletion and blocking of nonspecific sites were performed for 1 h on 2 wells coated
167 with PBS 2 % bovine serum albumin (BSA) for round 1 and 3 and with PBS 2%
168 skimmed milk for round 2. Phages were then incubated on the well coated with the
169 peptides for 2 h. Phages were washed 40 times with PBS 0.1 % Tween 20, with one
170 last wash in 50 mM Tris pH 8.0, 1 mM $CaCl_2$. For rounds 1 and 2, phage elution was

171 performed in the latter buffer containing 125 µg/mL bovine trypsin (Sigma-Aldrich, St.
172 Louis, MO, USA), for 15 min at room temperature. For round 3, phages were eluted
173 using 1.5 mM peptide in PBS pH 7.4. *E. coli* TG1 bacterial cells were used for phage
174 amplification. Ninety-six randomly chosen clones among the selected clones from
175 round 3 were sequenced (Azenta, Cambridge, MA, USA). Sequences were aligned,
176 clustered and compared from one selection condition to the others. Sequences
177 common to at least 2 selection conditions were considered as non-specific.

178 - *Cell culture and plasmid transfections*

179 Human Embryonic Kidney 293A (HEK293A) cells, HEK293/ΔGαs (a cell line depleted
180 for Gαs protein) (22) and HEK293/ΔGαs/q/11/12/13 (23) were cultured in Dulbecco's
181 Modified Eagle Medium DMEM (Eurobio, Les Ulis, France) supplemented with 10%
182 (v/v) foetal bovine serum, 100 IU/mL penicillin, 0.1 mg/mL streptomycin (Eurobio, Les
183 Ulis, France) and kept at 37°C in a humidified 5% CO_2 incubator. Cells were transiently
184 transfected in suspension using the Metafectene Pro transfection reagent (Biontex
185 Laboratories, München, Germany) following the manufacturer's protocol. For
186 interaction Bioluminescence resonance energy transfer (BRET) experiments, cells
187 were transiently co-transfected with plasmids encoding the human FSHR C-terminally
188 fused to the luciferase from the sea pansy *Renilla reniformis* (RLuc8) (0.1 µg plasmid
189 DNA/cm^2) as BRET donor, and increasing quantities of plasmids encoding the intra-
190 VHH C-terminally fused to the Venus GFP derivative with a G4S linker as BRET
191 acceptor (from 0 to 0.5 µg plasmid/cm^2) (Supplementary figure 2A). To have an
192 equivalent level of plasmid DNA transfected in all conditions, a pcDNA3.1 vector
193 (Invitrogen, Waltham, Massachusetts, USA) encoding Venus alone was co-
194 transfected. Further experiments were conducted with an excess of VHH plasmid DNA
195 (0.45 µg DNA/cm^2 of either T31-Venus or iPRC1-Venus plasmid) in addition to
196 plasmids encoding human FSHR-RLuc8, human AVPR2-RLuc8, human AVPR1A-
197 RLuc8, human AVPR1B-RLuc8, human CXCR4-RLuc8 or human PTH1R-RLuc8.
198 Forty-eight hours following transfection, HEK293A cells were stimulated with either 3.3
199 nM FSH, 100 nM AVP, 250 nM SDF1α (Preprotech, Neuilly-sur-Seine, France) or 10
200 nM PTH (Bachem, Bubendiorf, Switzerland) according to the transiently expressed
201 receptor, in presence of coelenterazine H. For Mini Gs protein (mGs, minimal
202 engineered GTPase domain of the Gα subunit) recruitment BRET experiments, cells
203 were transiently co-transfected with plasmids encoding the human FSHR-Rluc8 (0.1

204 µg plasmid DNA/cm^2), the NES-Venus-mGs (65 ng plasmid DNA/cm^2, kindly provided
205 by Pr. Nevin A. Lambert, Augusta University, Augusta, GA, USA) (24,25), and VHH-
206 6xHis (0.2 µg plasmid DNA/cm^2) (Supplementary figure 2B). For HTRF and flow
207 cytometry experiments, 0.5 ng Flag-tagged human FSHR (26) or 0.25 ng Flag-tagged
208 human AVPR2 (27) plasmid DNA/cm^2 and 80 ng of VHH-6xHis plasmid DNA/cm^2 were
209 used for transfection. For the condition without transfected VHH, an empty pcDNA3.1
210 plasmid was used. For confocal microscopy, two quantities of intra-VHH-Venus were
211 tested for transfection (0.3 or 0.45 µg plasmid DNA/cm^2). For Gαs protein competition,
212 HEK293/ΔGαs/q/11/12/13 were transfected with 0.1 µg DNA/cm^2 of FSHR-RLuc8
213 plasmid DNA, 0.25 µg DNA/cm^2 of Venus-mGs or iPRC1-Venus plasmid DNA, and 0.5
214 µg DNA/cm^2 of either empty pcDNA3.1 or Gαs protein plasmid DNA.

215 - *Peptide competition by HTRF*

216 Biotinylated peptides corresponding to FSHR ICL1, ICL2 and ICL3 (Genecust, Boynes,
217 France) as previously defined, and non-biotinylated competing decapeptides ICL3-Nt
218 (HIYLTVRNPN), ICL3-Mid (NPNIVSSSSD) and ICL3-Ct (SSSDTRIAKR) (GenScript
219 Biotech, Piscataway, New Jersey, USA) were used. One hundred and twenty µM of a
220 biotinylated peptide, with or without 1 mM of competing peptide were added to 30 nM
221 of purified bacterially-expressed VHHs in PBS 0.1% Tween 20 (PBS-T), and incubated
222 overnight at 4°C and 30 rpm. Background signal was obtained with PBS-T
223 supplemented with equivalent amount of DMSO as the other conditions. The sensors,
224 MAb Anti-6His-Tb cryptate (Cisbio, Waltham, Massachusetts, USA) and Streptavidin-
225 d2 (Cisbio, Waltham, Massachusetts, USA) were added following manufacturer's
226 protocol, and after a 1-hour incubation in the dark, fluorescence measurement was
227 performed with a TriStar² LB 942 Multimode Microplate Reader (Berthold Technologies
228 GmbH & Co., Wildbad, Germany).

229 - *In silico docking*

230 The model of the iPRC1 VHH was generated by homology modelling using SWISS-
231 MODEL (28–31). Docking of the iPRC1 CDR3 on the ICL3 of either inactive FSHR
232 (PDB: 812H) or activated FSH-FHSR-Gs complex (PDB: 812G) was performed using
233 the standard 'EASY' access settings on HADDOCK 2.4 (32,33). The generated
234 HADDOCK models were visualised, superimposed onto each other, and analysed
235 using the PyMOL Molecular Graphics System, Version 2.0 Schrödinger, LLC.

236 - *Data analysis*

237 Data were representative of at least 3 independent experiments and were expressed
238 as mean values ± SD. Data were analyzed and plotted using Graphpad Prism 9
239 (Graphpad Software Inc., San Diego, CA, USA). For interaction BRET, nonspecific
240 signal (when no VHH-Venus was expressed) was subtracted of the signal obtained
241 with T31 or iPRC1, and data were then normalized to T31 and fitted to a specific
242 binding curve with Hill slope (Graphpad Prism 9). For Mini Gs protein recruitment,
243 BRET data were expressed as a percentage of the maximal FSH-induced response in
244 the absence of VHH, and fitted to a one-phase association curve (Graphpad Prism 9).
245 For HTRF cAMP accumulation assay, data were normalized to forskolin-induced cAMP
246 accumulation and expressed as a percentage of ligand-induced response in the
247 absence of intra-VHH. For competing peptides HTRF, signal was normalized to
248 background and expressed as a percentage of iPRC1-ICL3 interaction signal.
249 Statistical significance was estimated by the Mann-Whitney test to compare 2 different
250 samples. Differences among means were considered significant at $P < 0.05$. Image
251 processing was performed with Fiji (34).

252 - *Data availability*

253 The nucleotide sequence of iPRC1 has been deposited in Genbank with accession
254 number OR554885

255

256 **Results**

257 ***Selection of the iPRC1 intra-VHH***

258 To select intra-VHH targeting the FSHR intracellular side, we performed phage display
259 on peptides corresponding to intracellular loops 1, 2 and 3 (ICL1, ICL2 and ICL3) of
260 the receptor (Figure 1). Following three rounds of selection, the common clones
261 identified in several conditions were considered as non-specific. Among the clones not
262 common to ICL1 and ICL2 selections, a VHH directed against the FSHR ICL3, iPRC1,
263 was selected through further analysis. An irrelevant intra-VHH, T31, randomly picked
264 from a llama phage library and consistently observed as devoid of FSHR binding, has
265 been used as a negative control in all following experiments.

266 ***Expression of iPRC1 in mammalian cells***

267 In order to be functionally characterized, iPRC1 and T31 were transiently expressed in
268 HEK293A cells. We first assessed potential aggregation of the T31-Venus and iPRC1-
269 Venus intra-VHHs (Figure 2A). Using confocal microscopy, we detected no sign of
270 aggregation but rather homogeneous expression of both intra-VHHs, even with high
271 quantities of transfected plasmid DNA (450 ng of DNA per cm^2). Then the expression
272 level of the two intra-VHH C-terminally linked to a 6xHis-tag was assessed by flow
273 cytometry (Figure 2B), in all conditions of the following functional assays. Control and
274 iPRC1 intra-VHHs both exhibited comparable levels of expression.

275 ***iPRC1 binding to the FSHR***

276 Even though iPRC1 was selected on the FSHR ICL3, it was crucial to confirm its
277 binding to the full-length receptor in native conditions. Here, the interaction between
278 iPRC1 and the human FSHR was assayed by a BRET method using the VHH C-
279 terminally fused to the Venus BRET acceptor, and the FSHR or the arginine-
280 vasopressin 2 receptor (AVPR2) fused to the RLuc8 BRET donor. With increasing
281 amounts of transfected VHH-Venus plasmids (Figure 3A), a dose-dependent and
282 much higher binding of iPRC1 to FSHR than to AVPR2 was observed, even though a
283 weak binding signal was detected with AVPR2. There was no impact of the presence
284 of the ligand on iPRC1 binding, which indicates that iPRC1 has no preference for
285 inactive or ligand-induced active conformations of the FSHR. The maximum binding

286 estimated from fitting the data to specific binding curves with Hill slope showed a
287 statistically significant difference for FSHR, when compared to AVPR2 (Figure 3B).
288 The interaction of iPRC1 with other class A GPCRs (AVPR1A, AVPR1B or CXCR4) or
289 a class B GPCR (PTH1R) was also evaluated with a single high quantity of intra-VHH
290 (Figure 3C). All these GPCRs showed an interaction signal close to AVPR2, thus
291 highlighting the specificity of iPRC1 for FSHR. Interestingly, PTH1R contains a BBxxB
292 basic motif similar to the FSHR. This motif that has been reported to be important in
293 Gs coupling to the FSHR (35). Hence, the possibility that this motif could be the iPRC1
294 epitope can be ruled out.
295 To confirm the interaction between iPRC1 and the FSHR ICL3 *in vitro*, the interaction
296 between FSHR ICL1, ICL2 or ICL3 peptides and purified iPRC1 was assessed by
297 HTRF (Figure 3D). No interaction was visualized between iPRC1 and ICL1 or ICL2,
298 but as expected, a strong signal was observed with ICL3. In order to further identify
299 the iPRC1 epitope, the interaction of iPRC1 with ICL3 was assessed in presence of
300 competing decapeptides covering ICL3 Nt part (ICL3-Nt), middle part (ICL3-Mid) and
301 Ct part (ICL3-Ct) (Figure 3D). A significant inhibition of interaction was obtained with
302 the ICL3-Mid peptide, suggesting that iPRC1 epitope likely encompasses amino acids
303 ^{558}NPNIVSSSSD^{567}. In the 3D-structure of the activated FSHR (PDB: 8I2G), the
304 NPNIV motif appears as a flexible loop that is constrainted between the extra-
305 membrane helices formed by ^{552}IYLTVR^{557} in Nt and by ^{563}SSSDTRI^{570} in Ct. Hence,
306 being the most exposed, this pentapeptide is the most likely epitope of iPRC1.

307 ***Functional effect of iPRC1 on ligand-induced G protein-dependent signalling***

308 Knowing that ICL2 and ICL3 are important interfaces between Gα proteins and class
309 A GPCRs (6), we focused on G protein-dependent signalling. In order to predict
310 whether iPRC1 would interfere with the Gs protein/ FSHR interaction, we first
311 performed docking studies of a modelled iPRC1 CDR3 on the ICL3 of human FSHR
312 active or inactive structures. Docking of the iPRC1 CDR3 on the inactive FSHR led to
313 9 clusters, the best one consisting of 83 models, having HADDOCK score of -89.1 +/-
314 5.9 (Figure 4A). The HADDOCK score is the weighted sum of energies, with the most
315 negative values representing the most energetically favourable models. Although only
316 the CDR3 of iPRC1 was defined as the active residues in the interaction during the
317 docking process, the models generated also suggested the involvement of CDR1 and
318 CDR2. Visual inspection of models indicated several poses of iPRC1 with varying

319 vertical-horizontal orientations located on the external side of ICL3 (Figure 4A, left, for
320 a focused view, see Supplementary Figure 3). The superimposition of the best models
321 from the different clusters onto the FSH-FSHR-Gs complex indicated that the binding
322 of iPRC1 to ICL3 would cause steric clash with Gαs (Figure 4A, right, for a focused
323 view, see Supplementary Figure 3). The degree of steric clash with Gαs varied
324 according to the orientation of iPRC1, being minimized with the horizontal pose.
325 However, such horizontal poses could incur steric clashes with the cell membrane.
326 Steric hindrance between iPRC1 and Gs, and the cell membrane, was also confirmed
327 with the active FSH-FSHR-Gs complex, as the models generated did not provide good
328 HADDOCK scores: the best cluster consisted of only 17 models with HADDOCK score
329 of -1.6 +/- 25.1. Overall, it is clear from these models that iPRC1 was either targeting
330 intra-membrane portions of the FSHR or was in steric clash with the cell membrane.
331 Since these docking data suggest a competition between G proteins and iPRC1 upon
332 FSH binding, we next investigated whether iPRC1 would impact ligand-induced G
333 protein-dependant second messenger production. The outcome of iPRC1 or T31
334 intracellular expression was assayed on cAMP production that results from G protein
335 recruitment upon receptor activation, using HTRF (Figure 4). When compared to the
336 mock-transfected condition (no VHH transfected), iPRC1 induced a decrease of 33%
337 of cAMP accumulation in HEK293A cells transiently co-expressing the FSHR and the
338 intra-VHH, and stimulated for 15 min with 0.3 nM FSH. No effect of the T31 control
339 was observed in the same conditions (Figure 4B). The selectivity of iPRC1 was tested
340 on two other Gs-coupled class A GPCRs, structurally unrelated to the FSHR, the
341 AVPR2 and the beta 2 adrenergic receptor (ADRB2). The AVP-induced cAMP
342 production in HEK293A cells transiently expressing AVPR2, and stimulated for 15 min
343 with 0.25 nM AVP (Figure 4C), or the ISO-induced cAMP production in HEK293A cells
344 endogenously expressing ADRB2 (Figure 4D) were not altered by the co-expression
345 of T31 as expected, nor of iPRC1. These data show that iPRC1 negatively regulates
346 the FSH-induced Gs protein-dependent signalling, and this effect is specific of the anti-
347 FSHR intra-VHH selected in this study.

348 As suggested by the docking data, the reduced cAMP production in response to FSH
349 might be due to iPRC1 partially preventing Gs protein interaction with the receptor. To
350 verify this hypothesis, we assessed the recruitment of Mini Gs to the receptor in
351 absence or in presence of T31 or iPRC1 by BRET (Figure 4E). This experiment was

352 performed in HEK293/ΔGαs to avoid competition with the endogenous untagged Gs
353 proteins. The intracellular expression of iPRC1 slightly decreased Mini Gs/FSH-
354 activated FSHR BRET signal in comparison to T31 or mock conditions, but not
355 significantly, as shown by the comparison of the estimated maximal mGs binding
356 (Figure 4F). These results suggest that iPRC1 does not compete with Gs for interaction
357 with FSHR. However, to confirm this point, we investigated whether an excess of Gαs
358 could displace iPRC1-Venus from FSHR-RLuc8 in HEK293 cells depleted of
359 Gs/q/11/12/13. No difference in iPRC1–FSHR interaction was observed. In contrast,
360 as expected, an excess of Gαs strongly displaced Venus-mGs interaction with the
361 FSHR. These results support the hypothesis that iPRC1 and Gαs do not compete for
362 FSHR binding.

363

364 **Discussion**

365 In this study, we have selected the first intra-VHH targeting a member of the
366 glycoprotein hormone receptor family, the FSHR, while only few VHHs targeting the
367 intracellular side of GPCRs have been functionally characterized to date. This intra-
368 VHH is directed against the FSHR ICL3 and impairs the cAMP production of the ligand-
369 bound receptor, despite the proper recruitment of Gαs. Thus, iPRC1 behaves as an
370 allosteric modulator of FSHR.

371 We first showed that iPRC1 was correctly expressed in mammalian cells and did not
372 aggregate, which makes it well suited for experiments in a cellular context. iPRC1
373 specifically recognized the FSHR, when compared to other GPCR, Gs-coupled or not.
374 However, iPRC1 specificity towards the two other glycoprotein hormone receptors,
375 LHCGR and TSHR, which share high sequence similarity with the FSHR, still remains
376 to be reported. Importantly, iPRC1 recognised the receptor whether it is FSH-
377 stimulated or not. Hence, iPRC1 is not specific of an inactive or an FSH-activated
378 conformation of the FSHR.

379 G proteins are recruited to the FSHR notably through the ERW motif present on ICL2,
380 but also through a basic motif on ICL3 (21) (Supplementary Figure 4). We showed that
381 iPRC1 does not bind the PTH1R, a GPCR that contains a basic motif similar to the
382 FSHR's. Even though these data suggest that this motif is not part of iPRC1 epitope,
383 iPRC1 might interfere with G protein interaction with the FSHR through steric

384 hindrance. This hypothesis is supported by our docking model that overall suggests
385 direct steric clashes with Gαs. Consistently, iPRC1 specifically reduced the FSH-
386 induced cAMP production in HEK293 cells transiently expressing the FSHR, but not
387 the AVPR2 or the ADRB2 in the presence of their respective ligands.

388 From our results, we anticipated a competition between iPRC1 and G proteins for
389 interaction with the receptor. Surprisingly, when the recruitment of mini Gs to the FSHR
390 was assayed in HEK293 cells depleted of Gαs protein, there was no significant impact
391 of the expression of iPRC1. The affinity of iPRC1 for the FSHR probably being weaker
392 than the affinity of G proteins for the receptor, the binding equilibrium might be in favour
393 of the G proteins. To further investigate if iPRC1 and full Gαs protein are in competition
394 for FSHR recruitment, iPRC1 interaction to the receptor was assessed in HEK293 cells
395 depleted for Gs/q/11/12/13 proteins, in presence of overexpressed Gαs. The latter was
396 not able to displace iPRC1, while it strongly displaced mGs binding, confirming that
397 iPRC1 and Gαs are likely able to bind FSHR simultaneously.

398 ICL3 is an allosteric site of major interest to modulate GPCR activity and downstream
399 signalling (36). This view probably applies to the FSHR since the recently solved FSHR
400 cryo-EM structure reveals a 14,9 Å movement of the N-term portion of TM6 helix,
401 suggesting the major importance of ICL3 in FSHR activation (16). Therefore, by
402 targeting ICL3, iPRC1 might affect FSHR helix conformational transitions, hence
403 activation. According to the docking studies, an interesting model for the action of
404 iPRC1 would be its binding to the external side of ICL3 in a horizontal pose. Whilst
405 steric clashes with Gαs is minimized, the presence of the iPRC1 however limits the
406 shift of the TM6 to allow for the full recruitment of Gαs since it would be blocked by the
407 cell membrane. This hypothesis is consistent with the binding data suggesting that
408 iPRC1 is able to interact with both active and inactive conformation of FSHR. The Gs
409 protein could also be recruited to the FSHR, but iPRC1 would imply a reorientation that
410 might not be optimal for its activation, thus explaining the reduction of cAMP
411 production. Interestingly, activation of Gαs is accompanied by a prominent shift of helix
412 5 away from its catalytic domain (6), a movement that may be hindered by the presence
413 of iPRC1. Furthermore, we show that the epitope of iPRC1 overlaps amino acids N^{558}
414 to D^{567} of FSHR ICL3. Yet, according to the recently described structure of the active
415 Gαs-coupled FSHR stabilized with compound 716340, where the ICL3 structure is
416 resolved, amino acid S^{566} engages an interaction with Y^{358} of the Gαs protein (16) (PDB

8I2G). This interaction would be disrupted by iPRC1, giving a possible explanation for partial activation of the Gαs protein.

The ICL3 length exhibits striking diversity among GPCRs, ranging from 10 to 240 amino-acids, and it has been recently proposed that this length might explain G protein selectivity (36), the shorter the loop, the lower the selectivity. In this view, when bound to the FSHR, whose ICL3 is only 23 amino acids long (against 47 and 55 amino acids for AVPR2 and ADRB2 respectively), iPRC1 might promote coupling to other G proteins.

ICL3 being also involved in the interaction of the receptor with β-arrestins, it would be of interest to study the impact of iPRC1 on β-arrestin-dependent signalling, for example through direct β-arrestin recruitment.

Since it does not preferentially interact with an inactive or active conformation of the FSHR, this intra-VHH is also a valuable tool to track FSHR trafficking in gonadal cells, which has never been done before. In addition, an intra-VHH stabilizing a conformation of specific interest could be used in reverse pharmacology. By stabilizing selective conformations of a GPCR with an intra-VHH, it would be possible to screen and identify extracellular binders that stabilize that same conformation and would be suited for therapeutics purposes (37).

Ligand binding to its cognate GPCR results in a series of conformational changes that propagate through the transmembrane domains, allowing the transmission of an extracellular signal to the intracellular compartments of the cell. Although intra-VHH have been instrumental to provide precious structural data on GPCRs, the extreme complexity of GPCR signalling in correlation with conformational changes has not been unravelled. Even though many published structures of GPCRs are available, domains such as the ICLs are unstructured, thus preventing any prediction of structure/ activity relationships. Therefore, intra-VHHs that bind to ICLs and interfere with GPCR signalling pathways constitute valuable tools to help complete structure/ activity studies performed so far.

Acknowledgements

The authors would like to acknowledge the Merck company for kindly providing purified recombinant human FSH, Pierre Martineau (Institut de Recherche en Cancérologie de Montpellier, France) for precious technical indications and for kindly providing the pCANTAB 6 phagemid vector and the KM13 helper phage.

Funding sources and disclosure of conflicts of interest

This work was funded with the support of Institut National de la Recherche Agronomique et de l'Environnement (INRAE), of the MAbImprove Labex (ANR-10-LABX-53) and of Région Centre Val de Loire ARD2020 Biomédicaments SELMAT grant and APR-IR INTACT grant.

PR was funded by a joint fellowship from Région Centre Val de Loire and INRAE PHASE Department. OV was funded by the APR-IR INTACT grant. AV, CaG and VJ was funded by the SELMAT grant of Région Centre Val de Loire ARD2020 Biomédicaments Program. CaG is co-funded by the INTACT grant from Région Centre Val de Loire. TB, ChG, GB and ER are funded by INRAE, FJ-A, NS and PC are funded by the Centre National de la Recherche Scientifique (CNRS).

466 **References**

467 1. Latorraca NR, Venkatakrishnan AJ, Dror RO. GPCR Dynamics: Structures in Motion. Chem
468 Rev. 2017; 117(1): 139-55. doi: 10.1021/acs.chemrev.6b00177

469 2. De Pascali F, Ayoub MA, Benevelli R, Sposini S, Lehoux J, Gallay N, et al. Pharmacological
470 Characterization of Low Molecular Weight Biased Agonists at the Follicle Stimulating
471 Hormone Receptor. Int J Mol Sci. 2021; 22(18): 9850. doi: 10.3390/ijms22189850

472 3. Stijlemans B, Conrath K, Cortez-Retamozo V, Van Xong H, Wyns L, Senter P, et al.
473 Efficient Targeting of Conserved Cryptic Epitopes of Infectious Agents by Single domain
474 Antibodies. J Biol Chem. 2004; 279(2):1256-61. doi:10.1074/ jbc.M307341200

475 4. Liu H, Schittny V, Nash MA. Removal of a Conserved Disulfide Bond Does Not
476 Compromise Mechanical Stability of a VHH Antibody Complex. Nano Lett. 2019; 19(8):
477 5524-9. doi: 10.1021/ acs.nanolett.9b02062

478 5. Manglik A, Kobilka B. The role of protein dynamics in GPCR function: insights from the
479 β2AR and rhodopsin. Curr Opin Cell Biol. 2014; 27: 136-43. doi: 10.1016/
480 j.ceb.2014.01.008.

481 6. Rasmussen SGF, Choi HJ, Fung JJ, Pardon E, Casarosa P, Chae PS, et al. Structure of a
482 nanobody-stabilized active state of the β2 adrenoceptor. Nature 2011; 469 (7329):
483 175-80. doi: 10.1038/ nature09648

484 7. Kruse AC, Ring AM, Manglik A, Hu J, Hu K, Eitel K, et al. Activation and allosteric
485 modulation of a muscarinic acetylcholine receptor. Nature 2013; 504 (7478): 101-6. doi:
486 10.1038/ nature12735

487 8. Huang W, Manglik A, Venkatakrishnan AJ, Laeremans T, Feinberg EN, Sanborn AL, et al.
488 Structural insights into μ-opioid receptor activation. Nature 2015; 524 (7565): 315-21.
489 doi: 10.1038/ nature14886

490 9. Masureel M, Zou Y, Picard LP, van der Westhuizen E, Mahoney JP, Rodrigues JPGLM, et
491 al. Structural insights into binding specificity, efficacy and bias of a β2AR partial agonist.
492 Nat Chem Biol. 2018; 14 (11): 1059-66. doi: 10.1038/ s41589-018-0145-x

493 10. Staus DP, Strachan RT, Manglik A, Pani B, Kahsai AW, Kim TH, et al. Allosteric nanobodies
494 reveal the dynamic range and diverse mechanisms of G protein-coupled receptor
495 activation. Nature 2016; 535 (7612): 448-52. doi: 10.1038/ nature18636

496 11. Irannejad R, Tomshine JC, Tomshine JR, Chevalier M, Mahoney JP, Steyaert J, et al.
497 Conformational biosensors reveal GPCR signalling from endosomes. Nature 2013; 495
498 (7442): 534-8. doi: 10.1038/ nature12000

499 12. Raynaud P, Gauthier C, Jugnarain V, Jean-Alphonse F, Reiter E, Bruneau G, et al.
500 Intracellular VHHs to monitor and modulate GPCR signaling. Front Endocrinol. 2022; 13:
501 1048601. doi: 10.3389/ fendo.2022.1048601

502 13. Staus DP, Wingler LM, Strachan RT, Rasmussen SGF, Pardon E, Ahn S, et al. Regulation of
503 β_2 -Adrenergic Receptor Function by Conformationally Selective Single-domain
504 Intrabodies. Mol Pharmacol. 2014; 85 (3): 472-81. doi: 10.1124/ mol.113.089516

505 14. McMahon C, Baier AS, Pascolutti R, Wegrecki M, Zheng S, Ong JX, et al. Yeast surface
506 display platform for rapid discovery of conformationally selective nanobodies. Nat Struct
507 Mol Biol. 2018; 25 (3): 289-96. doi: 10.1038/ s41594-018-0028-6

508 15. Gromoll J, Simoni M, Nordhoff V, Behre HM, De Geyter C, Nieschlag E. Functional and
509 clinical consequences of mutations in the FSH receptor. Mol Cell Endocrinol. 1996; 125
510 (1-2): 177-82. doi: 10.1016/ s0303-7207(96)03949-4

511 16. Duan J, Xu P, Zhang H, Luan X, Yang J, He X, et al. Mechanism of hormone and allosteric
512 agonist mediated activation of follicle stimulating hormone receptor. Nat Commun.
513 2023; 14 (1): 519. doi: 10.1038/ s41467-023-36170-3

514 17. Marion S, Robert F, Crepieux P, Martinat N, Troispoux C, Guillou F, et al. G Protein-
515 Coupled Receptor Kinases and Beta Arrestins Are Relocalized and Attenuate Cyclic 3′,5′-
516 Adenosine Monophosphate Response to Follicle-Stimulating Hormone in Rat Primary
517 Sertoli Cells. Biol Reprod. 2002; 66 (1): 70-6. doi: 10.1095/ biolreprod66.1.70

518 18. Marion S, Kara E, Crepieux P, Piketty V, Martinat N, Guillou F, et al. G protein-coupled
519 receptor kinase 2 and β-arrestins are recruited to FSH receptor in stimulated rat primary
520 Sertoli cells. J Endocrinol. 2006; 190 (2): 341-50. doi: 10.1677/ joe.1.06857

521 19. Reiter E, Lefkowitz RJ. GRKs and beta-arrestins: roles in receptor silencing, trafficking and
522 signaling. Trends Endocrinol Metab. 2006; 17 (4): 159-65. doi: 10.1016/
523 j.tem.2006.03.008

524 20. Sposini S, Jean-Alphonse FG, Ayoub MA, Oqua A, West C, Lavery S, et al. Integration of
525 GPCR Signaling and Sorting from Very Early Endosomes via Opposing APPL1 Mechanisms.
526 Cell Rep. 2017; 21 (10): 2855-67. doi: 10.1016/ j.celrep.2017.11.023

527 21. Ulloa-Aguirre A, Zariñán T, Jardón-Valadez E, Gutiérrez-Sagal R, Dias JA. Structure-
528 Function Relationships of the Follicle-Stimulating Hormone Receptor. Front Endocrinol
529 2018. doi: 10.3389/ fendo.2018.00707

530 22. Stallaert W, Van Der Westhuizen ET, Schönegge AM, Plouffe B, Hogue M, Lukashova V, et
531 al. Purinergic Receptor Transactivation by the β_2 -Adrenergic Receptor Increases
532 Intracellular Ca^{2+} in Nonexcitable Cells. Mol Pharmacol. 2017; 91 (5): 533-44. doi:
533 10.1124/ mol.116.106419

534 23. Devost D, Sleno R, Pétrin D, Zhang A, Shinjo Y, Okde R, et al. Conformational Profiling of
535 the AT1 Angiotensin II Receptor Reflects Biased Agonism, G Protein Coupling, and
536 Cellular Context. J Biol Chem. 2017; 292 (13): 5443–56. doi 10.1074/ jbc.M116.763854

537 24. Ayoub MA, Landomiel F, Gallay N, Jégot G, Poupon A, Crépieux P, et al. Assessing
538 Gonadotropin Receptor Function by Resonance Energy Transfer-Based Assays. Front
539 Endocrinol. 2015; 6. doi: 10.3389/ fendo.2015.00130

540 25. Wan Q, Okashah N, Inoue A, Nehmé R, Carpenter B, Tate CG, et al. Mini G protein probes
541 for active G protein–coupled receptors (GPCRs) in live cells. J Biol Chem. 2018; 293 (19):
542 7466-73. doi: 10.1074/ jbc.RA118.001975

543 26. Tranchant T, Durand G, Gauthier C, Crépieux P, Ulloa-Aguirre A, Royère D, et al.
544 Preferential β-arrestin signalling at low receptor density revealed by functional
545 characterization of the human FSH receptor A189 V mutation. Mol Cell Endocrinol. 2011;
546 331 (1): 109-18. doi: 10.1016/ j.mce.2010.08.016

547 27. Heitzler D, Durand G, Gallay N, Rizk A, Ahn S, Kim J, et al. Competing G protein-coupled
548 receptor kinases balance G protein and β-arrestin signaling. Mol Syst Biol. 2012; 8 (1):
549 590. doi: 10.1038/ msb.2012.22

550 28. Schindelin J, Arganda-Carreras I, Frise E, Kaynig V, Longair M, Pietzsch T, et al. Fiji: an
551 open-source platform for biological-image analysis. Nat Methods. 2012; 9 (7): 676-82.
552 doi: 10.1038/ nmeth.2019

553 29. Bertoni M, Kiefer F, Biasini M, Bordoli L, Schwede T. Modeling protein quaternary
554 structure of homo- and hetero-oligomers beyond binary interactions by homology. Sci
555 Rep. 2017; 7 (1): 10480. doi: 10.1038/ s41598-017-09654-8

556 30. Bienert S, Waterhouse A, de Beer TAP, Tauriello G, Studer G, Bordoli L, et al. The SWISS-
557 MODEL Repository—new features and functionality. Nucleic Acids Res. 2017; 45 (D1):
558 D313-9. doi: 10.1093/ nar/ gkw1132

559 31. Waterhouse A, Bertoni M, Bienert S, Studer G, Tauriello G, Gumienny R, et al. SWISS-
560 MODEL: homology modelling of protein structures and complexes. Nucleic Acids Res.
561 2018; 46 (W1): W296-303. doi: 10.1093/ nar/ gky427

562 32. Studer G, Rempfer C, Waterhouse AM, Gumienny R, Haas J, Schwede T. QMEANDisCo—
563 distance constraints applied on model quality estimation. Bioinformatics. 2020; 36 (6):
564 1765-71. doi: 10.1093/ bioinformatics/ btaa058

565 33. Van Zundert GCP, Rodrigues JPGLM, Trellet M, Schmitz C, Kastritis PL, Karaca E, et al. The
566 HADDOCK2.2 Web Server: User-Friendly Integrative Modeling of Biomolecular
567 Complexes. J Mol Biol. 2016; 428(4): 720-5. doi: 10.1016/ j.jmb.2015.09.014

568 34. Honorato RV, Koukos PI, Jiménez-García B, Tsaregorodtsev A, Verlato M, Giachetti A, et
569 al. Structural Biology in the Clouds: The WeNMR-EOSC Ecosystem. Front Mol Biosci.
570 2021; 8: 729513. doi: 10.3389/ fmolb.2021.729513

571 35. Timossi C, Ortiz-Elizondo C, Pineda DB, Dias JA, Conn PM, Ulloa-Aguirre A. Functional
572 significance of the BBXXB motif reversed present in the cytoplasmic domains of the human
573 follicle-stimulating hormone receptor. Mol Cell Endocrinol. 2004; 223 (1–2): 17–26.
574 doi:10.1016/ j.mce.2004.06.004

575 36. Sadler F, Ma N, Ritt M, Sharma Y, Vaidehi N, Sivaramakrishnan S. Autoregulation of GPCR
576 signalling through the third intracellular loop. Nature 2023; 615 (7953): 734-41. doi:
577 10.1038/ s41586-023-05789-z

578 37. Pardon E, Betti C, Laeremans T, Chevillard F, Guillemyn K, Kolb P, et al. Nanobody-
579 Enabled Reverse Pharmacology on G-Protein-Coupled Receptors. Angew Chem Int Ed. 2018;
580 57 (19): 5292-5. doi: 10.1002/ anie.201712581

581

582 **Figure legends**

583 **Figure 1**: ***iPRC1 selection workflow*.** A phage library was constructed following llama
584 immunization by injection of a cDNA encoding the hFSHR. Selection was done by
585 phage display on the peptides corresponding to the FSHR intracellular loops, ICL1,
586 ICL2 and ICL3. Ninety-six randomly selected clones were sequenced for each
587 condition, and after cross-comparison, specific VHHs were selected.

588 **Figure 2*: iPRC1 and irrelevant T31 intra-VHH expression in HEK293A cells*. (A)**
589 Confocal microscopy representative images of T31-Venus (a and b) and iPRC1-Venus
590 (c and d) (in green) transiently expressed in HEK293A cells, using two quantities of
591 plasmid DNA (b and d). Cell nuclei were stained with Hoechst solution (in blue). **(B)**
592 Flow cytometry histograms showing the population of cells expressing either the
593 irrelevant intra-VHH T31-6xHis or iPRC1-6xHis (in red) in comparison to "mock"-cells
594 transfected with empty pcDNA3.1 vector (in blue).

595 **Figure 3**: ***iPRC1 associates to the FSHR, whether FSH is present or not.* (A)**
596 Bioluminescence resonance energy transfer (BRET) binding assay between FSHR-
597 RLuc8 and increasing amounts of transfected iPRC1-Venus plasmid. Experiments
598 were done in the absence of ligand or in the presence of 3.3 nM FSH or 100 nM AVP,
599 as indicated. BRET ratios (at 2 min following FSH addition) were normalized to the
600 BRET ratios obtained in the presence of the irrelevant T31-Venus intra-VHH. Data are
601 represented as mean ± SD, and the curves correspond to fitted data to specific binding
602 curves with Hill slope, N=4. **(B)** Comparison of the estimated maximum binding
603 obtained for iPRC1 to the FSHR to the estimated maximum binding values obtained
604 for iPRC1 association to AVPR2. Data are represented as mean ± SD. Statistical
605 significance was assessed by unpaired Mann-Whitney test, N = 4, * $p < 0.05$. **(C)** BRET
606 binding assay between FSHR-RLuc8, AVPR2-RLuc8, AVPR1A-RLuc8, AVPR1B-
607 RLuc8, CXCR4-RLuc8 or PTH1R-RLuc8 and a fixed amount of iPRC1-Venus plasmid.
608 HEK293A cells were stimulated with either 3.3 nM FSH, 100 nM AVP, 250 nM SDF1α
609 or 10 nM PTH according to the receptor. BRET ratios after 1 min of stimulation were
610 normalized to the BRET ratios obtained in the presence of the irrelevant T31-Venus
611 intra-VHH. Data are represented as mean ± SD, N=3. **(D)** iPRC1 and ICL1, ICL2 or
612 ICL3 peptides interaction and iPRC1-ICL3 interaction using competing peptides ICL3-
613 Nt, ICL3-Mid and ICL3-Ct by HTRF. Data are normalized to background signal,

614 expressed as the percentage of iPRC1-ICL3 interaction signal and represented as
615 mean ± SD, N=3.

616 **Figure 4**: ***iPRC1 expression affects G protein signalling pathway.*** **(A)** iPRC1 CDR3
617 molecular docking to hFSHR ICL3. *Left:* Models of inactive FSHR (PDB: 8I2H) with 2
618 examples of iPRC1 poses. Right: Models of inactive FSHR (PDB: 8I2H)-iPRC1
619 superimposed onto FSHR-FSH-Gαs (PDB: 8I2G) (for simplicity, FSH, Gβ, Gγ and
620 Nb35 are not shown). Homogeneous time-resolved fluorescence (HTRF) cAMP
621 accumulation assay in HEK293A cells transiently expressing the AVPR2 **(B)** or FSHR
622 **(C)** or endogenously expressing ADRB2 **(D)**, and transiently expressing either T31 or
623 iPRC1, stimulated with 0.25 nM AVP (N=4), 0.3 nM FSH (N=6) or 0.2 µM ISO (N=4)
624 for 15 min. For each receptor, data were normalized to the cAMP response to Fsk and
625 represented as the percentage of the cAMP response to FSH in the absence of
626 transfected VHH. Statistical significance between the mean ± SD was assessed by
627 unpaired Mann-Whitney test, N = 6, ** $p < 0.01$. **(E)** Bioluminescence resonance
628 energy transfer (BRET) assay measuring the recruitment of NES-Venus-mGs to
629 FSHR-RLuc8, in presence of either T31 or iPRC1, in response to cells stimulation with
630 33 nM FSH. BRET ratios are expressed as percentage of the maximal FSH-response
631 in the absence of VHH. Data are represented as mean ± SD, and curves correspond
632 to fitted data to one-phase association curves, N = 4. **(F)** Comparison of the estimated
633 maximum binding of Mini Gs proteins to the FSHR in presence of T31 or iPRC1. Data
634 are represented as mean ± SD. Statistical significance was assessed by unpaired
635 Mann-Whitney test, N = 4. **(G)** Interaction inhibition assay in HEK293 cells depleted of
636 Gs/q/11/12/13 transiently transfected with FSHR-RLuc8. iPRC1-Venus and Venus-
637 mGs were transiently expressed in absence (pcDNA3.1) or in presence of
638 overexpressed Gαs protein. Data are represented as mean ± SD (N = 3).

639

Figure 1

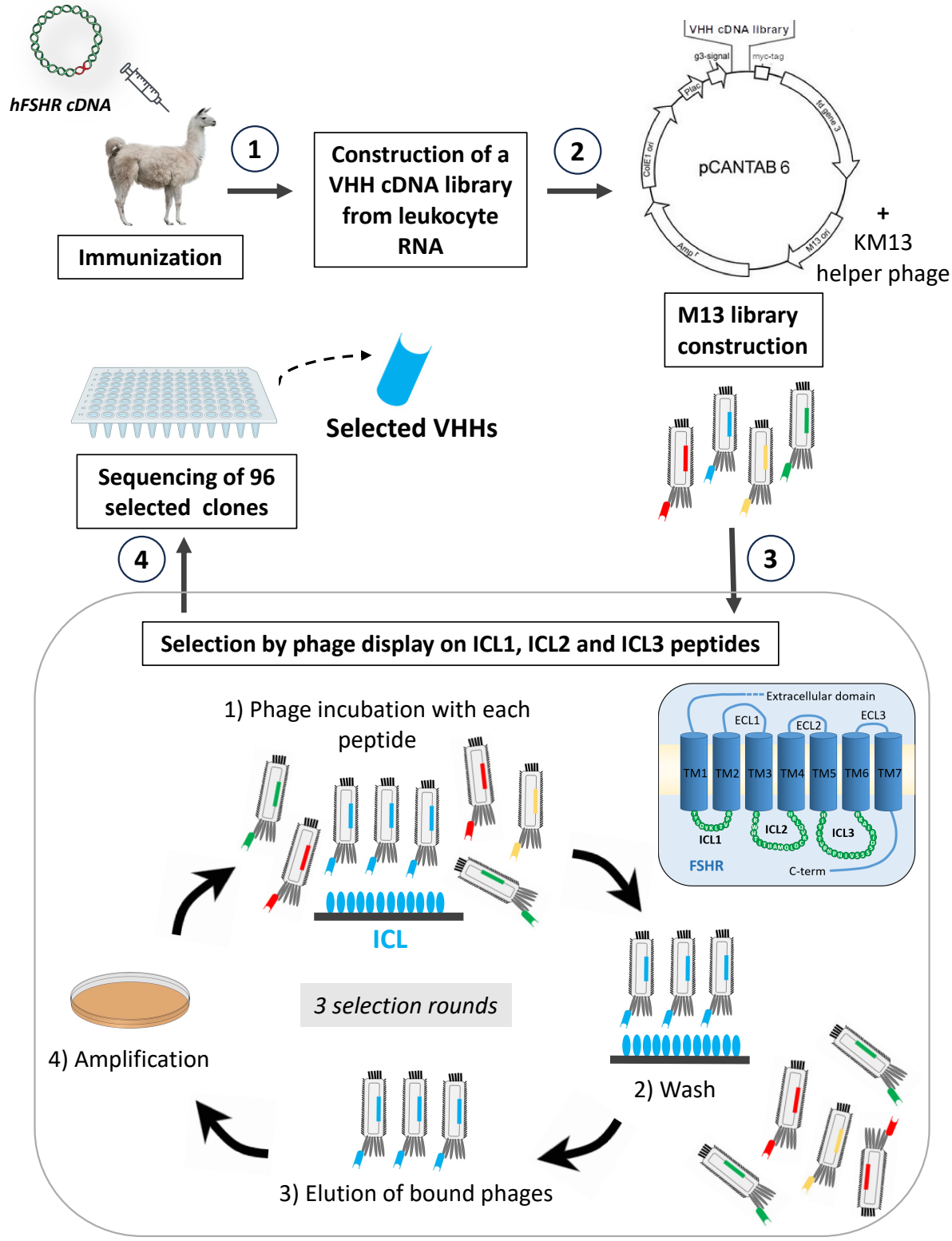

640

641

Figure 2

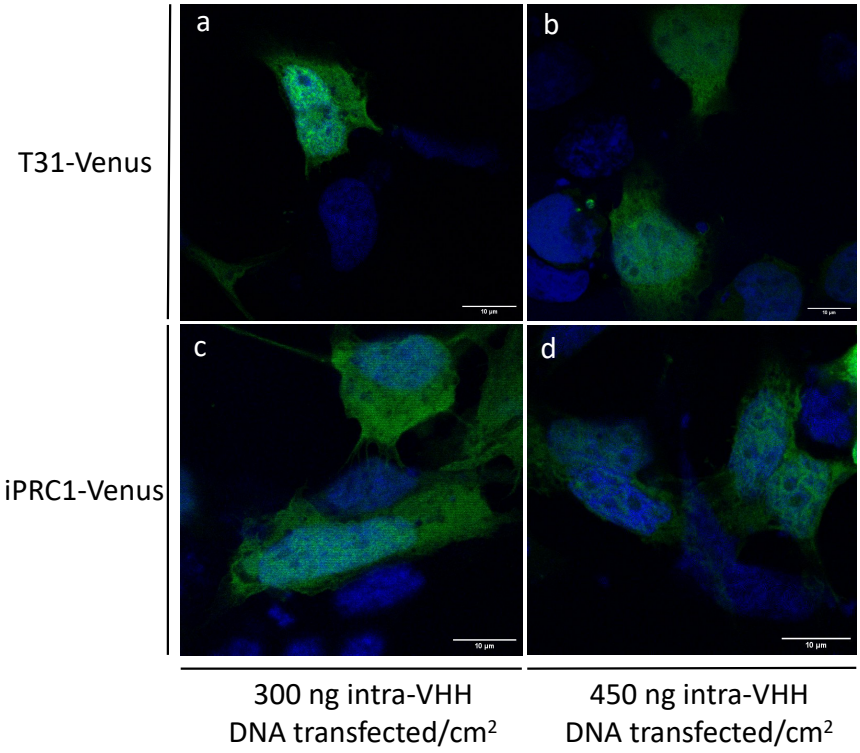

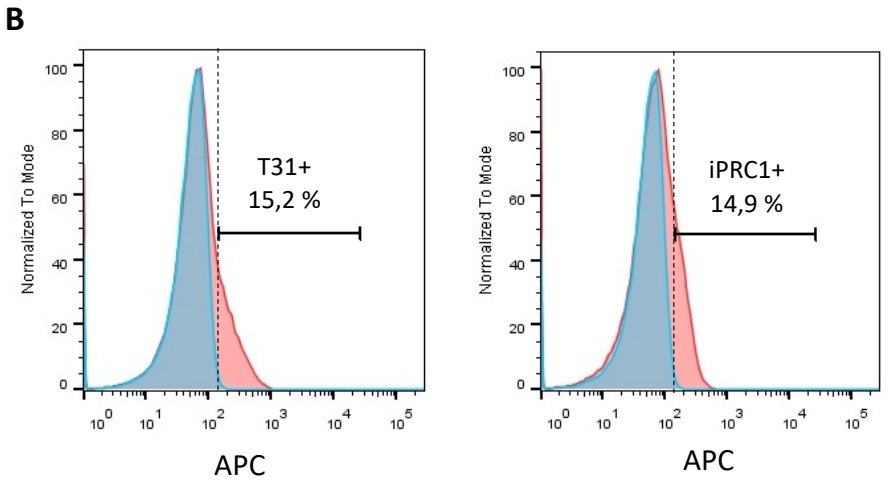

642

643

Figure 3

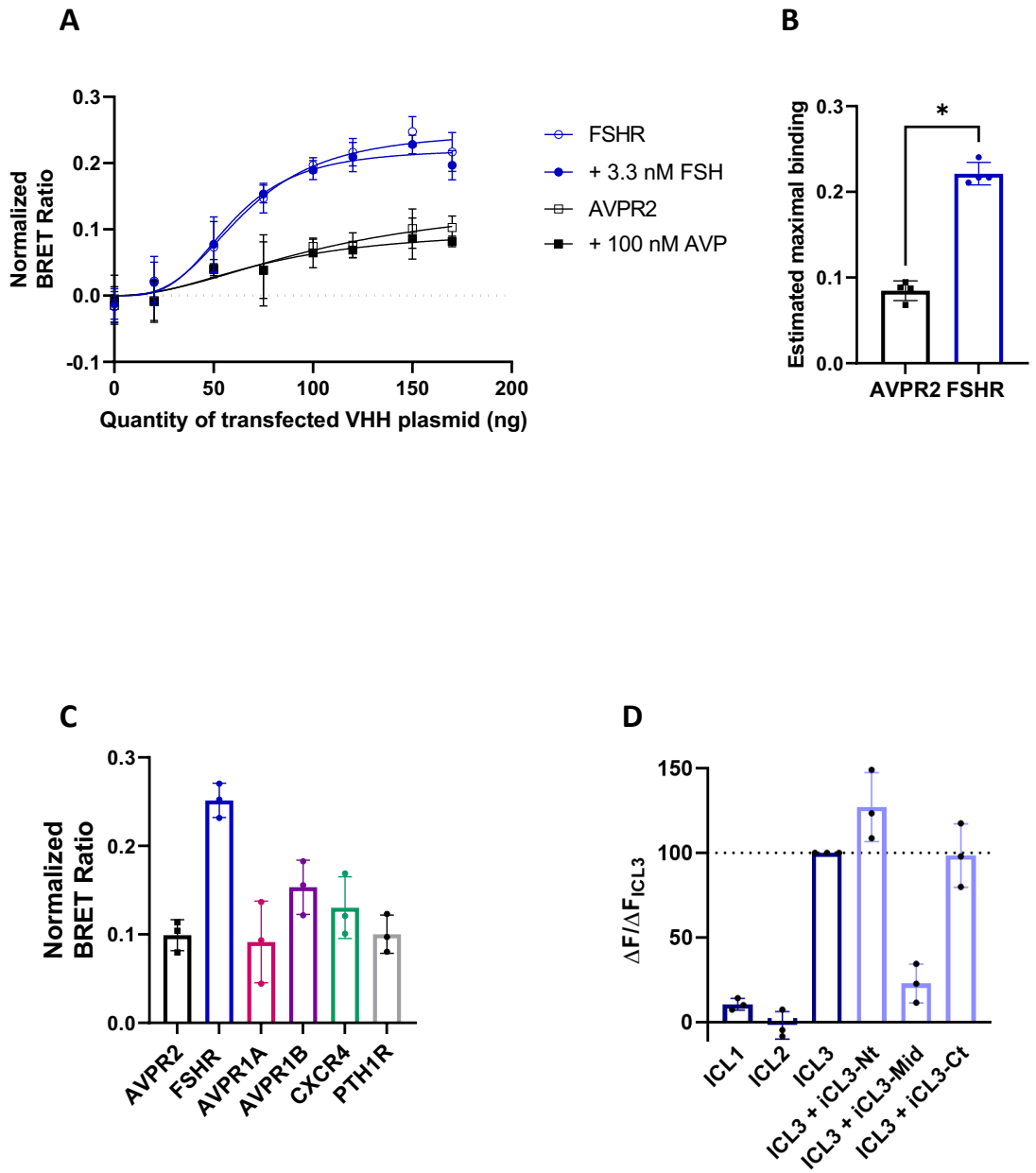

644

645

646

Figure 4

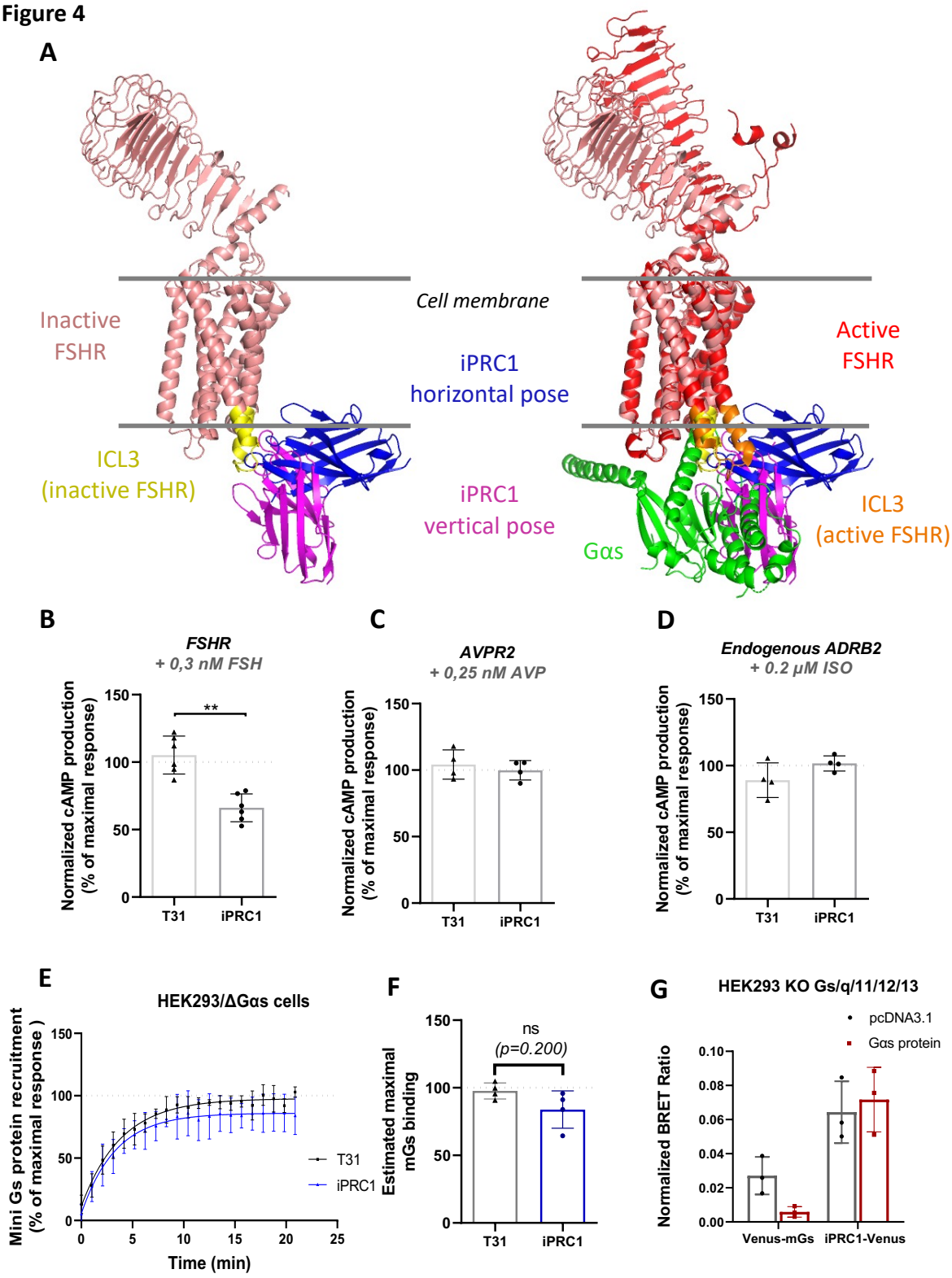

647

648

649

SUPPLEMENTARY

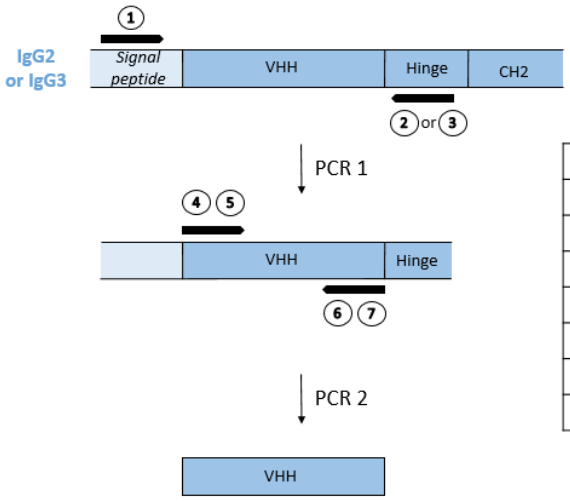

Primer	Sequence
1	5'-GGTGGTCCTGGCTGCTCT-3'
2	5'-TTGTGGTTTTGGTGTCTTGGG-3'
3	5'-GGGGTCTTCGCTGTGGTGCGC-3'
4	5'-GTCGTCGGCCCAGCCGGCCATGGCCGAGGTGCAGCTG-3'
5	5'-GTCGTCGGCCCAGCCGGCCATGGCCGAGGTGCAGCTGCAGGMGTCTGG-3'
6	5'-GCTGCTGCGGCCGCTGAGGAGACGGTGACCTGGGTCCC-3'
7	5'-GCTGCTGCGGCCGCTGAGGAGACGGTGACCTGGGT-3'

Supplementary figure 1: ***Phage library construction.*** cDNAs were subjected to a first PCR amplification to discriminate between IgG2 or IgG3 VHH cDNAs and IgG1 VH cDNAs. Two different PCR were performed using **1** as 5' primer and **2** or **3** specific of the IgG2 and IgG3 hinge regions respectively, as 3' primers. Four nested PCR were made on each first PCR product using primers encompassing the VHH coding sequence: **4** or **5** from the framework 1 domain as primer 5', and **6** or **7** from the framework 4 domain as 3' primer, including the restriction enzyme sites SfiI and NotI (underlined), respectively. The eight nested PCR products were pooled and inserted between the SfiI and NotI sites of the pCANTAB 6 phagemid vector (kindly provided by Pierre Martineau).

650

651

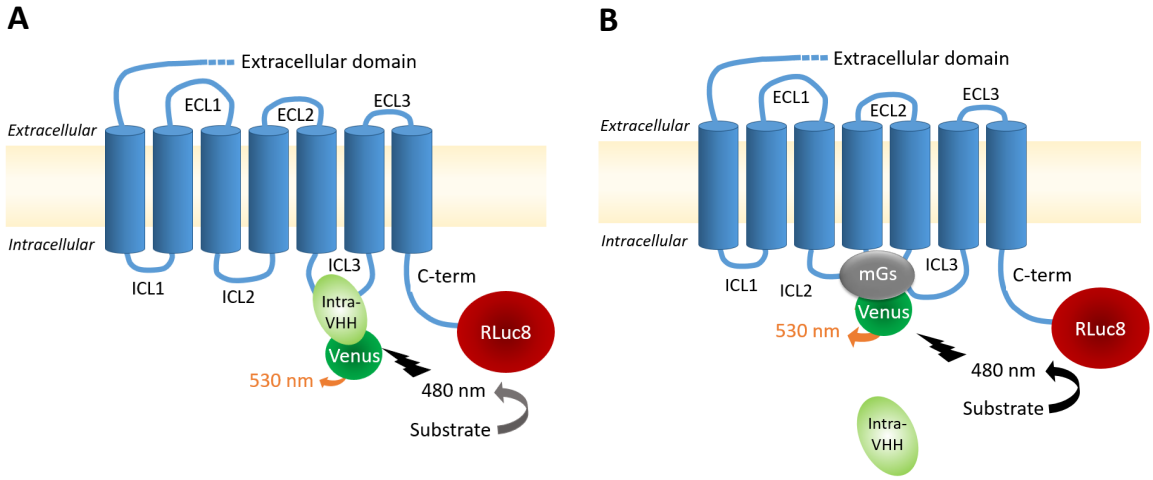

Supplementary figure 2: ***Schematic representation of BRET assays.*** The RLuc8 fused to FSHR metabolizes its substrate, thus producing a wave at 480 nm, which subsequently excites the Venus fused to the intra-VHH **(A)** or the Mini Gs **(B)** if nearby.

652

653

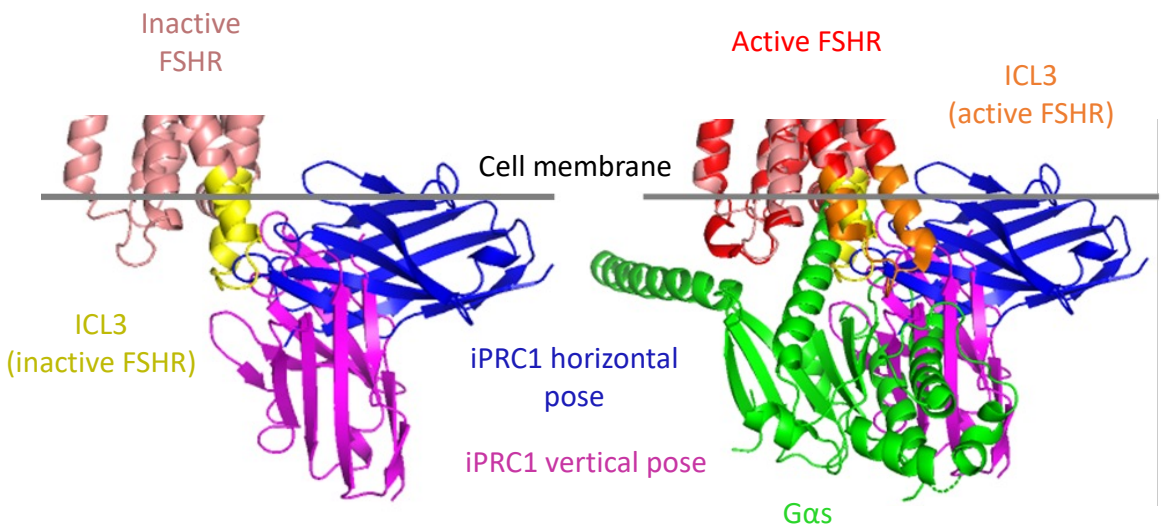

Supplementary figure 3: ***iPRC1 CDR3 molecular docking to the ICL3 at the intracellular side of hFSHR.*** *Left:* Models of inactive FSHR (PDB: 8I2H) with 2 examples of iPRC1 poses. *Right:* Models of inactive FSHR (PDB: 8I2H)-iPRC1 superimposed onto FSHR-FSH-Gαs (PDB: 8I2G) (for simplicity, Gβ, Gγ and Nb35 are not shown).

654

655

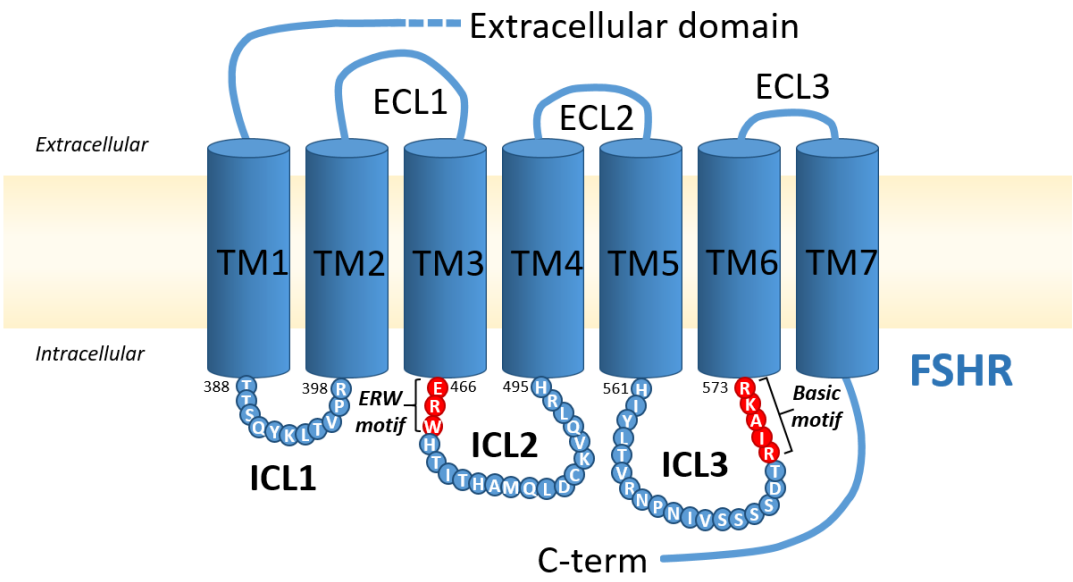

Supplementary figure 4: ***Sites of G protein binding on the FSHR.*** G proteins are notably recruited to FSHR through two motifs : the ERW motif located on the ICL2, and basic motif (BBXXB) located on the ICL3. *TM: transmembrane domain; ECL: extracellular loop; ICL: intracellular loop*

656

657

Item	Manufacturer	Reference
Agonists		
human FSH	Merck (Darmstadt, Germany)	
Isoproterenol	Sigma-Aldrich (St. Louis, MO, USA)	I6504
arginine-vasopressin	Tocris Bioscience (Noyal Châtillon sur Seiche, France)	2935/1
Forskolin	Sigma-Aldrich (St. Louis, MO, USA)	F6886
SDF1α	Preprotech (Neuilly-sur-Seine, France)	300-28A
PTH	Bachem (Bubendiorf, Switzerland	H-4835
Kits		
cAMP Gs dynamic kit	Cisbio (Waltham, Massachusetts, USA)	62AM4PEB
LeukoLOCK™ Fractionation & Stabilization Kit	Invitrogen (Waltham, Massachusetts, USA)	AM1933
Cytofix/Cytoperm™ Fixation/Permeabilization kit	BD Biosciences (Franklin Lakes, NJ, USA)	554714
MAb Anti-6HIS-Tb cryptate	Cisbio (Waltham, Massachusetts, USA)	61HISTLA
Streptavidin-d2	Cisbio (Waltham, Massachusetts, USA)	610SADLB
Cells		
E. coli TG1 bacteria	Cambrige Bioscience (Cambridge, UK)	60502-2
BL21 competent E. coli bacterial cells	New England BioLabs (Ipswich, Massachusetts, USA)	C2530H
Peptides		
human FSHR ICL1, ICL2, ICL3	Genecust (Chalmont, France)	
Biotinylated human FSHR ICL1, ICL2, ICL3	Genecust (Chalmont, France)	
human FSHR ICL3-Nt, ICL3-Mid, ICL3-Ct	GenScript Biotech (Piscataway, New Jersey, USA)	
Antibodies		
His antibody APC	Milteny Biotech (Bergisch Gladbach, Germany)	130-119-782
Chemicals		
BSA	Sigma-Aldrich (St. Louis, MO, USA)	A7906
Tween-20	Thermo Fisher Scientific (Waltham, MA, USA)	M12247
Tris	MP Biomedicals (Irvine, CA, USA)	819623
EDTA	Sigma-Aldrich (St. Louis, MO, USA)	E5134
Saccharose	Sigma-Aldrich (St. Louis, MO, USA)	2003349
$MgSO_4$	VWR Chemicals (Radnor, Pennsylvania, USA)	25165292
Cell culture and microscopy		
pcDNA3.1	Invitrogen (Waltham, Massachusetts, USA)	V79020
Bovine trypsin	Eurobio (Les Ulis, France)	CEZTDA00 0U
coelenterazine H	Interchim (Montluçon, France)	R3078C
DMEM	Eurobio (Les Ulis, France)	CM1DME68 01
fetal bovine serum	Eurobio (Les Ulis, France)	CVFSVF00 01
Penicillin/ Streptomycin	Eurobio (Les Ulis, France)	15140-122
Metafectene Pro transfection reagent	Biontex Laboratories (München, Germany)	T040-5.0
Poly-L-Lysine	Sigma-Aldrich (St. Louis, MO, USA)	P7280
HBSS w/o Ca^{2+} Mg^{2+}	Life Technologies (Marly-le-Roi, France)	14175095
Epredia™ Shandon™ Immu-Mount	Thermo Fisher Scientific (Waltham, MA, USA)	9990402
pET22b	Novagen, Merck KGaA (Darmstadt, Germany)	69744
2xYT	Thermo Fisher Scientific (Waltham, MA, USA)	22712020
Ampicillin	Thermo Fisher Scientific (Waltham, MA, USA)	11593027
IPTG	Sigma-Aldrich (St. Louis, MO, USA)	I6758
Protino Ni-NTA 1 mL FPLC column	Macherey-Nagel, Hoerdt, France	745410.5
Cytometry		
FcR Blocking Reagent human	Miltenyi Biotech (Bergisch Gladbach, Germany)	130-059-901
LIVE/DEAD™ Fixable Violet Dead Cell Stain	Invitrogen (Waltham, Massachusetts, USA)	L23105
Softwares		
ZEN software	Zeiss (Oberkochen, Germany)	
FlowJo software	FlowJo (Ashland, OR, USA)	
Graphpad Prism 9	Graphpad Software Inc. (San Diego, CA, USA)	

Supplementary Table 1: ***References of the materials.***

658